



## Frequency and voltage dependence of electrical conductivity, complex electric modulus, and dielectric properties of Al/Alq<sub>3</sub>/p-Si structure

İkram ORAK<sup>1,\*</sup> , Abdulkemim KARABULUT<sup>2</sup> 

<sup>1</sup>Vocational School of Health Services, Bingöl University, Bingöl, Turkey

<sup>2</sup>Faculty of Engineering, Department of Electrical and Electronics Engineering, Sinop University, Sinop, Turkey

Received: 24.07.2019

Accepted/Published Online: 07.01.2020

Final Version: 12.02.2020

**Abstract:** In order to enhance the capacitance of the Al/p-Si metal-semiconductor structure, the Alq<sub>3</sub> thin film was coated between these two layers using the spin coating technique as the interlayer. The electrical conductivity, real and imaginary parts of electric modulus, dielectric loss and dielectric constant parameters were examined at the room temperature by the help of admittance measurements in the 100 kHz to 1 MHz frequency range. The effect of frequency on the dielectric constant and dielectric loss values is negligible at the negative voltage values, up to about 0.8 V, and these values rapidly ascended after 0.8 V. The function of electrical modulus complex has been examined from the point of permittivity and impedance in order to clutch the contribution of the particle border on the relaxation mechanism of the materials. It is established that the examined dielectric parameters strongly correlated with the voltage and frequency. As a result, the changes in the dielectric parameters and electrical modulus due to the varying frequency were described as the results of relaxation process, polarization and surface conditions. Furthermore, it could be stated that the Alq<sub>3</sub> material used in the interfacial layer is a useful material which could be used in addition to the conventional materials.

**Key words:** Dielectric properties, spin coating, Al/Alq<sub>3</sub>/p-Si, frequency and voltage dependency

### 1. Introduction

Semiconductor-based devices are being used in many different electronic applications with new developments [1–4]. In particular, the use of high dielectric materials have become obligatory to satisfy the need for new structures that can improve the quality and performance of the manufactured devices and adjust their capacitive properties [5–9]. Generally, in order to improve the electrical performances of diode-based devices, materials having high dielectric properties such as HfO<sub>2</sub>, Al<sub>2</sub>O<sub>3</sub>, TiO<sub>2</sub> or organic/inorganic materials have been utilized in place of traditional SiO<sub>2</sub>, which is known as low dielectric material [10–15]. In this context, it is possible to enhance the devices having the high performance and desired properties with organic materials placed between metal and semiconductor layer.

Alq<sub>3</sub> organic material is considered to be one of the most remarkable organic materials due to being environmentally friendly, electrically high resistance, being produced at low temperatures and stability compared with many known oxide films. In addition to these, it has become a widely selected material in organic light emitting diodes due to its low molecular weight, strong luminescence properties and low cost, and it is also used as the base material for various dyes to adjust the emission color from green to red [16–18]. There are

\*Correspondence: ikramorak@gmail.com

many studies on the optical, structural, morphological, and photoluminescence properties of the synthesized Alq<sub>3</sub> film [19–21]. However, the electrical properties and the effect of annealing on the produced material were investigated [22]. Investigations on the Alq<sub>3</sub>-based devices have shown that the Alq<sub>3</sub> film is structurally stable and sensitive to light [23,24].

There are various techniques utilized to cover organic materials onto the desired substrate. When the advantages of the mentioned techniques are examined, spin coating technique stands out due to its great advantages such as homogeneity, enormous material combination and perfect control of processes. At the same time, it provides great convenience in experimental applications [25,26].

In our previous study [27], we investigated the temperature effects on the electrical parameters, photovoltaic characteristics, frequency and voltage effects on the capacitance and conductance characteristics and morphological properties of fabricated Al/Alq<sub>3</sub>/p-Si device. As a result of our studies, we have reported that the electrical properties of the produced devices are affected by temperature and it could be used in wide temperature applications [27]. We have also stated that it is sensitive to light and structurally stable. However, we have reported that the electrical characteristics of the produced device are strongly dependent on voltage and frequency. Besides the electrical properties of the devices, the dielectric properties is of great importance in order to reveal the detailed features of the device and to present the application areas more clearly. In this regard, we examined the varying voltage and frequency effect on the electrical conductivity, complex electric modulus, and dielectric properties of Al/Alq<sub>3</sub>/p-Si device in the current study.

## 2. Experimental details

The Al/Alq<sub>3</sub>/p-Si heterojunction-based device was produced by using Alq<sub>3</sub> interlayer and one-side polished silicon wafer. The silicon semiconductor substrate to be used in the device fabrication was bathed in acetone and propanol for approximately 7 min, respectively, and it was washed in DI water (with 18 MΩ.cm resistivity) for a required period and dried with nitrogen. After this step, the back side of Si was coated with Al metal, and under nitrogen gas atmosphere it was annealed for 3 min at 500 °C, thereby ohmic contact was completed. The prepared Alq<sub>3</sub> solution was coated on the nonohmic side by using spin coating method. The thickness of the coated interlayer in the fabricated device was about 94 nm, which was detected using the profilometer. In the next step, the prepared the Alq<sub>3</sub>-covered wafer was sheathed with aluminum thermally to ensure Schottky metal contact (0.5 mm radius and circular). The schematically illustration and energy band gap of the device are given in Figure 1. The frequency-dependent conductance and capacitance properties were carried out by the aid of HP 4192A LF impedance analyzer.

## 3. Results and discussion

The calculations of the complex electrical modulus and dielectric constant for a produced device are of great importance, and it is necessary to determine the distributions of the real and imaginary parts of these parameters against applied voltage and frequency variation [28]. The capacitance-conductance against the voltage measurements was performed in the range of 100–1000 kHz to examine these distributions. As is known, the complex permittivity is expressed as  $\varepsilon^* = \varepsilon' - j\varepsilon''$ , in this formula,  $j, \varepsilon'$  and  $\varepsilon''$  stands for the imaginary root, the real and imaginary parts of this complex, respectively. Besides, real and imaginary parts in the above equation could be formulated as follows [29,30]:

$$\varepsilon' = \frac{C_m}{C_i} = \frac{C_m d_i}{\varepsilon_0 A} \quad (1)$$

and

$$\varepsilon'' = \frac{G_m}{\omega C_i} = \frac{G_m d_i}{\omega \varepsilon_0 A} \quad (2)$$

in above formula, measured capacitance, thickness of coated interlayer, free space permittivity, contact area, measured conductance, and angular frequency are represented by  $C_m$ ,  $d_i$ ,  $\varepsilon_0$ ,  $A$ ,  $G_m$ , and  $\omega$  terms, respectively.

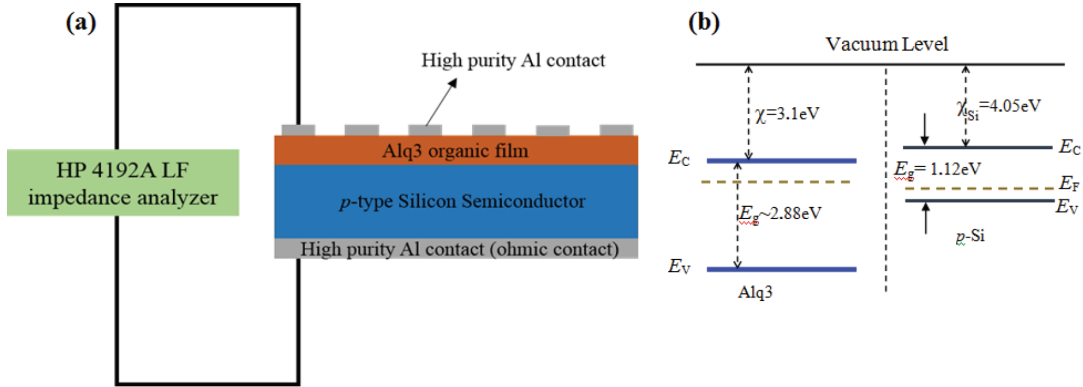


**Figure 1.** a) Schematically illustration of the Al/Alq<sub>3</sub>/p-type Si device, b) The energy band gap of Alq<sub>3</sub>/p-Si heterojunction.

The plotted real part of dielectric function (or dielectric constant)-voltage graph is presented in Figure 2. As seen in figure, the dielectric constant values are approximately the same up to 0 V and have not changed depending on the frequency. Then, there was a rapid increase in these values, and this increase was observed in all frequency values. Besides, the dielectric constant values decreased as the frequency increases, at positive voltage values.

Another important parameter, the imaginary part of the dielectric function, i.e. the dielectric loss, was calculated and its behavior against voltage was investigated. Dielectric loss could be defined as the phenomenon of bulk energy accumulation resulting from the imposition of a varying electric field in environments with dielectric loss characteristics. In other words, the dielectric loss could be expressed as the energy loss caused by the heating of a dielectric material in a variable electric field [31]. In Figure 3, the distribution of dielectric loss versus voltage is plotted for different frequencies. Dielectric loss values increase with increasing frequency for all voltage values. However, as seen in Figure 3, these values are less affected by frequency change in the negative voltage regions than the positive voltage regions. As seen from Figures 4 and 5, both parts of the dielectric function are influentially dependent on the voltage and frequency at high voltages. At the negative voltage region and the low positive voltage values, i.e. the inversion region, these values remain almost fixed. The behavior of these two parts of the dielectric function is related to their ability to follow the alternating current signal at low and high frequencies, and when the behavior of the real part of the function is examined, it is seen that the ability to follow the signal at low frequencies is stronger [32–35]. However, another reason for these behaviors is existence of the surface states and polarizations [35,36].

One of the crucial factors affecting the transmission mechanism of a produced device is its impedance characteristics. The behavior of this significant parameter against voltage was plotted for different frequencies and demonstrated in Figure 4. As seen in the figure, impedance values decreased by the increase of frequency. At the same time, these values decreased with increasing voltage and approach to a constant value towards to

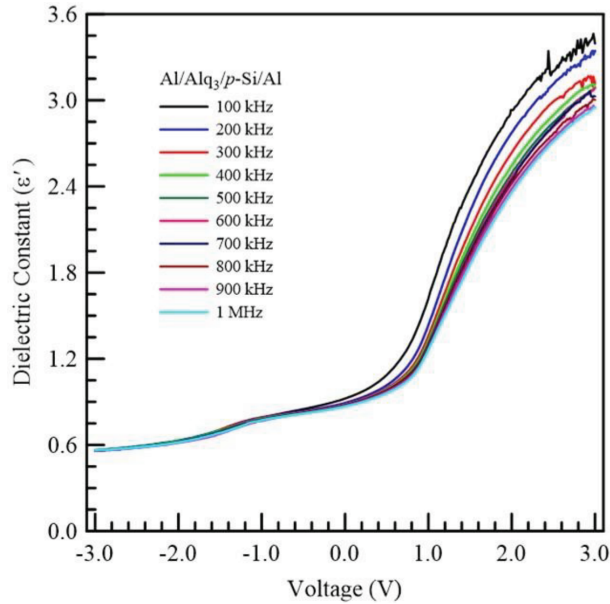


**Figure 2.** Voltage-dependent dielectric constant values of Al/Alq<sub>3</sub>/p-Si/Al heterojunction.

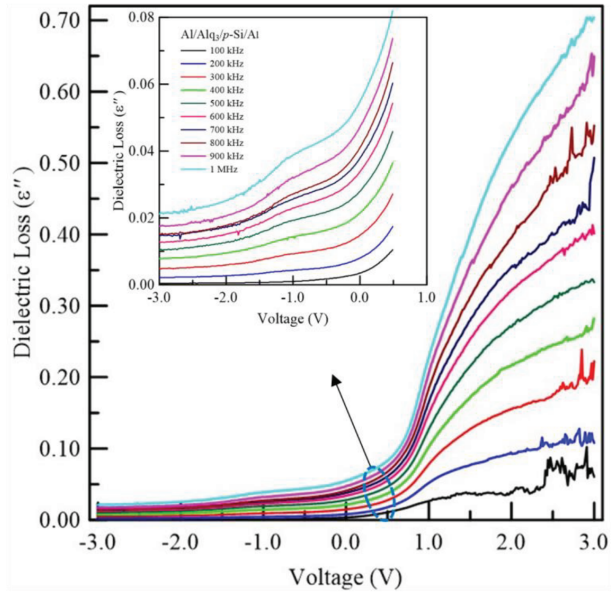


**Figure 3.** Voltage-dependent dielectric loss values of Al/Alq<sub>3</sub>/p-Si/Al heterojunction.

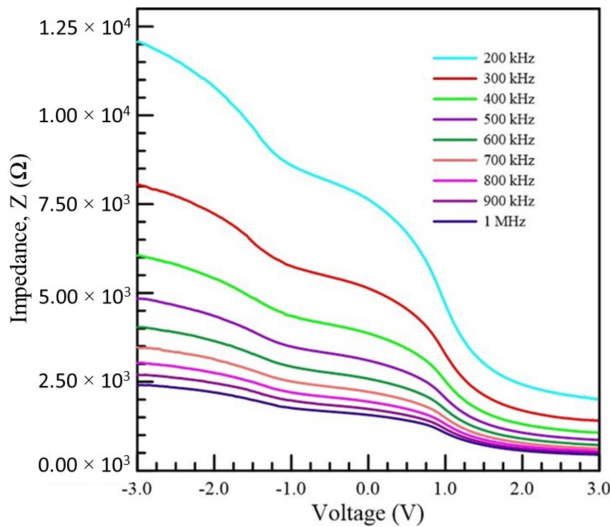


**Figure 4.** Impedance-voltage characteristics of Al/Alq<sub>3</sub>/p-Si/Al heterojunction.

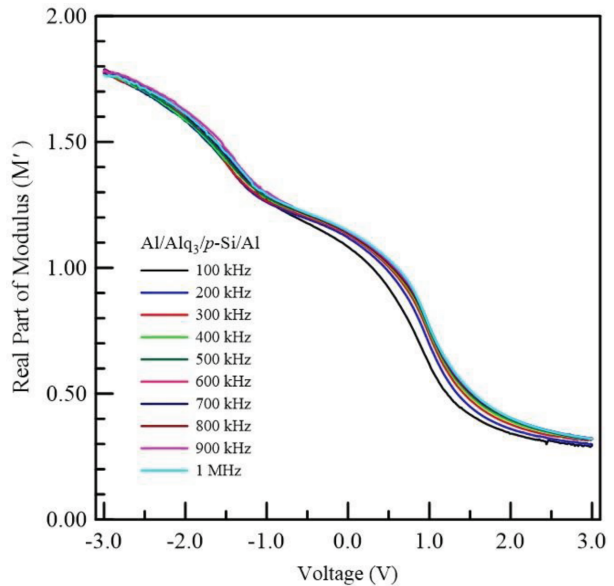


**Figure 5.** Frequency dependence of the real part of complex electric modulus of the Al/Alq<sub>3</sub>/p-Si/Al heterojunction for different voltages.

high voltage values. The impedance values were measured to be approximately  $1.20 \times 10^4 \ \Omega$  at  $-3$  volts and  $200$  kHz, while  $2.43 \times 10^3 \ \Omega$  at  $1$  MHz. In addition, it was determined as  $2.01 \times 10^3 \ \Omega$  for the frequency of  $200$  kHz at  $3$  V, and  $4.49 \times 10^2 \ \Omega$  for  $1$  MHz. The change in the impedance value is related to the presence of the movement paths of the mobility charge carriers [37,38]. The conductivity of the fabricated device was reduced by the increase of the impedance value at negative voltages, since the impedance and conductivity terms

are inversely proportional. In other words, the conductivity values of the device increased with the decreasing impedance in positive voltage region, and this situation could be attributed to the increasing of range of motion of the charge carriers as the voltage increased [39].

The electric field relaxation in the material physically contributes to the electric modulus to show the behavior of the real dielectric relaxation process. The material permittivity,  $\varepsilon^*$ , is inversely proportional to the complex electric modulus ( $M^*$ ), where  $M^* = M' + jM''$ . An alternative approach could be gained with the modulus to investigate the materials' electrical response and these already have been used by scientists to work on relaxation phenomena in organic/inorganic materials and ionic conductors [40]. Besides, the complex modulus contributes to the confirmation of the ambiguity that occurred due to the grain or grain boundary effect at elevated temperatures, which is not easy to distinguish in complex impedance plots [41]. As stated above,  $M^*$  is given by the inverse of complex permittivity and could be stated as follows [42]:

$$M^* = M' + jM'' = \frac{1}{\varepsilon^*} = \frac{\varepsilon'}{(\varepsilon')^2 + (\varepsilon'')^2} + j \frac{\varepsilon''}{(\varepsilon')^2 + (\varepsilon'')^2} \quad (3)$$

Figures 5 and 6 show that increase on the frequency increases  $M'$  and  $M''$ , which might be attributed to the polarization.  $M^*$  has been studied with regards to impedance and permittivity in order to understand the grain boundary contribution to the relaxation mechanism of the materials. Also, the study on the complex electric modulus gives a chance to examine the localized dielectric relaxation phenomenon and long-range conduction at microscopic level [43]. On the other hand, at high frequencies, the value shows a maximum point for each applied forward bias voltage because of the relaxation processes while  $M'$  and  $M''$  become zero at low frequencies [44]. The bulk traps and surface states may produce a charge effect since the traps and surfaces could store the charges and they release them once the appropriate external ac alternating voltage and forward applied bias are provided [45]. As a result, it could be safely stated that the exhibition of relaxation phenomena by the structure can be observed with the peak behavior in modulus or the variation in its characteristics with frequency.

The electrical modulus curves for Al/Alq<sub>3</sub>/p-Si/Al heterojunction, the imaginary part versus real part of modulus curves, for various frequencies were imparted in Figure 7. The analysis of the electrical modulus is utilized to detect electronic or ionic conductivity, i.e. to determine whether there is nonlocalized conduction or relaxation process [40]. On the other hand, it is a significant and appropriate method for evaluating, identifying, and interpreting the electrical transmission phenomena' dynamic aspects [46]. As seen in Figure 7, the mentioned curves are described by the existence of symmetrical and circle-like arcs of different magnitudes in the  $M'$  axis. The semicircle-like peaks observed in the figure indicate the existence of relaxation process. The minor semicircle-like peaks at low frequency match up to the contribution of the effects of low grain border. Contrary to this situation, the observed large semicircle-like peaks at high frequencies indicate that the grain borders or bulk have a large effect [47].

The behavior of the frequency-dependent ac electrical conductivity of the produced Al/Alq<sub>3</sub>/p-Si/Al heterojunction against the varying voltage was determined using the following formula [48,49]:

$$\sigma_{ac} = \left( \frac{d}{A} \right) \omega C \tan \delta = \omega \varepsilon'' \varepsilon_0 \quad (4)$$

It could be seen from Figure 8 that  $\sigma_{ac}$  values do not alter in the inversion region and the mentioned values increased sharply with increasing voltage for all frequencies in the accumulation region. As seen from the figure,

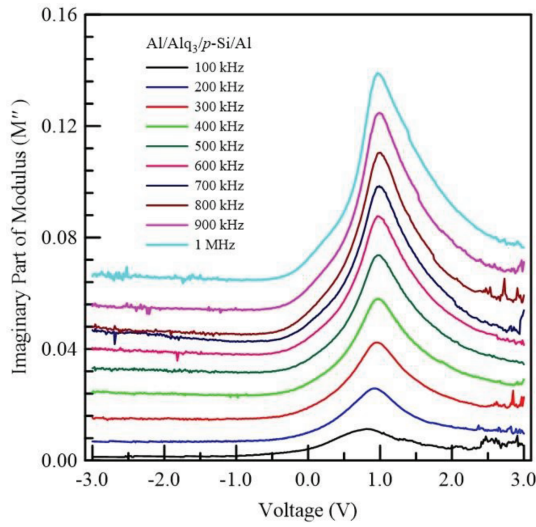


**Figure 6.** Frequency dependence of the imaginary part of complex electric modulus of the Al/Alq<sub>3</sub>/p-Si/Al heterojunction for different voltages.

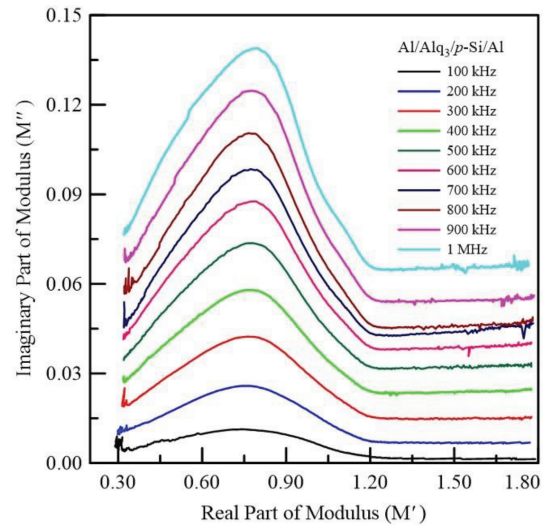


**Figure 7.** The real part of complex electric modulus versus the imaginary part of modulus of the Al/Alq<sub>3</sub>/p-Si/Al heterojunction for different frequencies.

the sharpness's of the variation in the conductivity values increases with increasing frequency, i.e. the change of values in the higher frequencies were greater than the low frequencies. These variations in the electrical conductivity are referred to dislocations or impurities, which ascribe at the grain borders that occur under circumstances beyond our control [50]. Furthermore, this alteration in the  $\sigma_{ac}$  leads to a rise in the eddy current, and this situation causes an increase in energy loss because of the decrease of series resistance [51]. The experimental results reveal that an organic/polymer interlayer placed between the semiconductor and the metal layers changes the surface conditions and the total series resistance of the structure, and could lead to significant alterations in the dielectric properties.

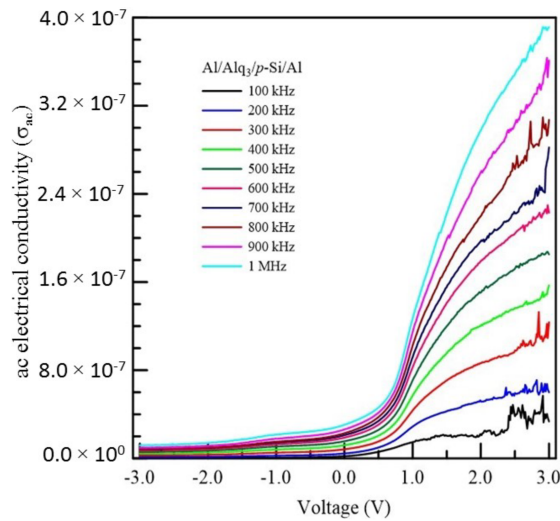


**Figure 8.** ac electric conductivity ( $\sigma_{ac}$ ) versus voltage plots of Al/Alq<sub>3</sub>/p-Si/Al heterojunction for different frequency values.

#### 4. Conclusions

In this study, in order to be able to define the dielectric features of Al/Alq<sub>3</sub>/p-Si device, the electrical conductivity, real and imaginary parts of electric modulus, dielectric loss, and dielectric constant parameters were examined at room temperature by the help of admittance measurements in the 100 kHz to 1 MHz frequency range. The experimental results showed that the device characteristics are strictly dependent on voltage and frequency. The real and imaginary portion of the dielectric function increased in the positive voltage region as the voltage increases, and was strongly influenced by the frequency, particularly in this region. While the actual value of the complex modulus function was not significantly affected by the frequency, it decreased as the voltage increased. At the same time, the imaginary value of the complex modulus function increased with increasing frequency, and showed peaks due to polarization and localized interface states at approximately 1 V. At low frequencies, the conductivity value becomes nearly independent of the frequency corresponding to dc conductivity, while at higher frequencies it increased with rising AC conductivity. As a result, the alterations that occurred in the dielectric characteristics owing to the variable frequency are defined as the result of polarization, surface conditions states and relaxation process. Besides, the produced metal-organic-semiconductor device can be used in energy storage applications due to the dielectric characteristics of the Alq<sub>3</sub> organic material.

#### References

- [1] Orak I, Kocyigit A, Turut A. The surface morphology properties and respond illumination impact of ZnO/n-Si photodiode by prepared atomic layer deposition technique. *Journal of Alloys and Compounds* 2017; 691: 873-879. doi: 10.1016/j.jallcom.2016.08.295
- [2] Sung MJ, Kim K, Kwon SK, Kim YH, Chung DS. Phenanthro [110, 9, 8-cdefg] carbazole-thiophene, donor–donor copolymer for narrow band green-selective organic photodiode. *The Journal of Physical Chemistry C* 2017; 121: 15931-15936. doi: 10.1021/acs.jpcc.7b04793
- [3] Al-Hazmi FE, Yakuphanoglu F. Photoconducting and photovoltaic properties of ZnO: TiO<sub>2</sub> composite/p-silicon heterojunction photodiode. *Silicon* 2018; 10: 781-787. doi: 10.1007/s12633-016-9530-9
- [4] Mohanraj K, Balasubramanian D, Chandrasekaran J, Babu B. Structural, morphological, optical and electrical properties of nail-shaped CdO nanoparticles synthesized by chemical route assisted microwave irradiation method for P–N junction diode application. *Journal of Materials Science: Materials in Electronics* 2017; 28: 7749-7759. doi: 10.1007/s10854-017-6470-0
- [5] Hanafy TA. Dielectric relaxation and alternating-current conductivity of gadolinium-doped poly (vinyl alcohol). *Journal of Applied Polymer Science* 2008; 108: 2540-2549. doi: 10.1002/app.27567
- [6] Karabulut A. Dielectric characterization of Si-based heterojunction with TiO<sub>2</sub> interfacial layer. *Iğdır Üniversitesi Fen Bilimleri Enstitüsü Dergisi* 2018; 8: 119-129. doi:10.21597/jist.418869
- [7] Gyanan MS, Kumar A. Tunable dielectric properties of TiO<sub>2</sub> thin film based MOS systems for application in microelectronics. *Superlattices and Microstructures* 2016; 100: 876- 885. doi: 10.1016/j.spmi.2016.10.054
- [8] Robertson J, Wallace RM. High-K materials and metal gates for CMOS applications. *Materials Science and Engineering: R: Reports* 2015; 88: 1-41. doi: 10.1016/j.mser.2014.11.001
- [9] Cherif A, Jomni S, Mliki N, Beji L. Electrical and dielectric characteristics of Al/Dy<sub>2</sub>O<sub>3</sub>/p-Si heterostructure. *Physica B:Condensed Matter* 2013; 429: 79-84. doi: 10.1016/j.physb.2013.07.026
- [10] Hacıoglu SO, Unlu NA, Aktas E, Hizalan G, Yildiz ED et al. A triazoloquinoline and benzodithiophene bearing low band gap copolymer for electrochromic and organic photovoltaic applications. *Synthetic Metals* 2017; 228: 111-119. doi:10.1016/j.synthmet.2017.04.017
- [11] Ali HAM, El-Zaidia EFM. Investigation of structural, electrical conductivity and dielectric properties of bulk Azure A chloride. *The European Physical Journal Plus* 2019; 134 (5): 188. doi: 10.1140/epjp/i2019-12559-4

- [12] Karabulut A, Orak İ, Türüt A. The photovoltaic impact of atomic layer deposited TiO<sub>2</sub> interfacial layer on Si-based photodiodes. *Solid-State Electronics* 2018; 144: 39-48. doi: 10.1016/j.sse.2018.02.016
- [13] Reddy MSP, Sreenu K, Reddy VR, Park C. Modified electrical properties and transport mechanism of Ti/p-InP Schottky structure with a polyvinylpyrrolidone(PVP) polymer interlayer. *Journal of Materials Science: Materials in Electronics* 2007; 28 (6): 4847-4855. doi: 10.1007/s10854-016-6131-8
- [14] Mohan VM, Weiliang Q, Jie S, Wen C. Electrical properties of poly (vinyl alcohol)(PVA) based on LiFePO<sub>4</sub> complex polymer electrolyte films. *Journal of Polymer Research* 17 2010; 1: 143-150. doi:10.1007/s10965-009-9300-0
- [15] Tataroğlu A, Ahmedova C, Barim G, Al-Sehemi AG, Karabulut A et al. Electronic and optoelectronic properties of Al/coumarin doped Pr<sub>2</sub>Se<sub>3</sub>-Ti<sub>2</sub>Se/p-Si devices. *Journal of Materials Science: Materials in Electronics* 2018; 29 (15): 12561-12572. doi: 10.1007/s10854-018-9372-x
- [16] Esaki Y, Matsushima T, Adachi C. Dependence of the amorphous structures and photoluminescence properties of tris (8-hydroxyquinolinato) aluminum films on vacuum deposition conditions. *Organic Electronics* 2019; 67: 237-241. doi: 10.1016/j.orgel.2019.01.032
- [17] Comandè F, Ansermet JP. Pulsed magnetic resonance of Alq<sub>3</sub> OLED detected by electroluminescence. *Synthetic Metals* 2013; 173: 40-42. doi:10.1016/j.synthmet.2012.12.037
- [18] Ahn JH, Lee JU, Kim TW. Impedance characteristics of ITO/Alq<sub>3</sub>/Al organic light-emitting diodes depending on temperature. *Current Applied Physics* 2007; 7 (5): 509-512. doi: 10.1016/j.cap.2006.10.012
- [19] Berleb S, Mückl AG, Brütting W, Schworer M. Temperature dependent device characteristics of organic light-emitting devices. *Synthetic Metals* 2000; 111: 341-344. doi: 10.1016/S0379-6779(99)00361-6
- [20] Tang CW, VanSlyke SA, Chen CH. Electroluminescence of doped organic thin films. *Journal of Applied Physics* 1989; 65 (9): 3610-3616. doi: 10.1063/1.343409
- [21] Gu J, Yin B, Fu S, Jin C, Liu X et al. Controlled Self-Assembly of Low-Dimensional Alq<sub>3</sub> Nanostructures from 1D Nanowires to 2D Plates via Intermolecular Interactions. *Electronic Materials Letters* 2018; 14 (2): 181-186. doi: 10.1007/s13391-018-0013-6
- [22] Farag AAM, Gunduz B, Yakuphanoglu F, Farooq WA. Controlling of electrical characteristics of Al/p-Si Schottky diode by tris (8-hydroxyquinolinato) aluminum organic film. *Synthetic Metals* 2010; 160 (23-24): 2559-2563. doi:10.1016/j.synthmet.2010.10.005
- [23] Gu J, Yin B, Fu S, Feng M, Zhang Z et al. Surface tension driven aggregation of organic nanowires via lab in a droplet. *Nanoscale* 2018; 10 (23): 11006-11012. doi: 10.1039/c8nr02592d
- [24] Riminucci A, Graziosi P, Calbucci M, Cecchini R, Prezioso M et al. Low intrinsic carrier density LSMO/Alq<sub>3</sub>/AlO<sub>x</sub>/Co organic spintronic devices. *Applied Physics Letters* 2018; 112 (14): 142401. doi: 10.1063/1.5006387
- [25] Sevgili Ö, Lafzi F, Karabulut A, Orak İ, Bayındır S. The synthesis of new bola-amphiphile TPEs and the comparison of current transformer mechanism and structural properties for Al/Bis (HCTA)-TPE/p-Si and Al/Bis (HCOA)-TPE/p-Si heterojunctions. *Composites Part B: Engineering* 2019; 172: 226-233. doi: 10.1016/j.compositesb.2019.05.020
- [26] Farooq WA, Elgazzar E, Dere A, Dayan O, Serbetci Z et al. Photoelectrical characteristics of novel Ru (II) complexes based photodiode. *Journal of Materials Science: Materials in Electronics* 2019; 30 (6): 5516-5525.
- [27] Karabulut A, Orak İ, CanlıS, Yıldırım N, Türüt A. Temperature-dependent electrical characteristics of Alq<sub>3</sub>/p-Si heterojunction. *Physica B: Condensed Matter* 2018; 550: 68-74. doi: 10.1016/j.physb.2018.08.029
- [28] Maril E, Tan SO, Altındal Ş, Uslu I. evaluation of electric and dielectric properties of Metal-Semiconductor structures with 2% GC-doped-(Ca<sub>3</sub>Co<sub>4</sub>Ga<sub>0.001</sub>O<sub>x</sub>) interlayer. *IEEE Transactions on Electron Devices* 2018; 65 (9): 3901-3908. doi: 10.1109/TED.2018.2859907
- [29] Sevgili Ö, Tasçioğlu I, Boughdachi S, Azizian-Kalandaragh Y, Altındal S. Examination of dielectric response of Au/HgS-PVA/n-Si (MPS) structure by impedance spectroscopy method. *Physica B Condensed Matter* 2019; 566: 125-135. doi: 10.1016/j.physb.2019.04.029



- [30] Demirezen S, Tanrıku EE, Altındal Ş. The study on negative dielectric properties of Al/PVA (Zn-doped)/p-Si (MPS) capacitors. *Indian Journal of Physics* 2019; 93 (6): 739-747. doi: 10.1007/s12648-018-1355-5
- [31] Mehdizadeh M, *Microwave/RF applicators and probes: for material heating, sensing, and plasma generation*. William Andrew, USA: Elsevier, 2015.
- [32] Karabulut A, Türüt A, Karataş Ş. The electrical and dielectric properties of the Au/Ti/HfO<sub>2</sub>/n-GaAs structures. *Journal of Molecular Structure* 2018; 1157: 513-518. doi:10.1016/j.molstruc.2017.12.087
- [33] Sattar AA, Rahman SA. Dielectric properties of rare earth substituted Cu-Zn ferrites. *Physica Status Solidi A* 2003; 200 (2): 415-422. doi: 10.1002/pssa.200306663
- [34] Tripathi R, Kumar A, Bharti C, Sinha TP. Dielectric relaxation of ZnO nanostructure synthesized by soft chemical method. *Current Applied Physics* 2010; 10 (2): 676-681. doi: 10.1016/j.cap.2009.08.015
- [35] Coşkun M, Polat Ö, Coşkun FM, Durmuş Z, Çağlar M et al. Frequency and temperature dependent electrical and dielectric properties of LaCrO<sub>3</sub> and Ir doped LaCrO<sub>3</sub> perovskite compounds. *Journal of Alloys and Compounds* 2018; 740: 1012-1023. doi: 10.1016/j.jallcom.2018.01.022
- [36] Bibi M, Abbas H, Baqi S. Outcome of temperature variation on sol-gel prepared CuO nanostructure properties (optical and dielectric). *Materials Chemistry and Physics* 2017; 192: 67-71. doi: 10.1016/j.matchemphys.2017.01.074
- [37] Kumari K, Prasad K, Choudhary RNP. Impedance spectroscopy of (Na<sub>0.5</sub>Bi<sub>0.5</sub>)(Zr<sub>0.25</sub>Ti<sub>0.75</sub>)O<sub>3</sub> lead-free ceramic. *Journal of Alloys and Compounds* 2008; 453(1-2): 325-331. doi: 10.1016/j.jallcom.2006.11.081
- [38] Omri A, Bejar M, Dhahri E, Es-Souni M, Valente MA et al. Electrical conductivity and dielectric analysis of La<sub>0.75</sub>(Ca,Sr)<sub>0.25</sub>Mn<sub>0.85</sub>Ga<sub>0.15</sub>O<sub>3</sub> perovskite compound. *Journal of Alloys and Compounds* 2012; 536: 173-178. doi: 10.1016/j.jallcom.2012.04.094
- [39] Wu IW, Wang PS, Tseng WH, Chang JH, Wu CI. Correlations of impedance-voltage characteristics and carrier mobility in organic light emitting diodes. *Organic Electronics* 2012; 13 (1): 13-17. doi: 10.1016/j.orgel.2011.09.016
- [40] Gogoi P, Srinivas P, Sharma P, Pamu D. Optical, dielectric characterization and impedance spectroscopy of Ni-substituted MgTiO<sub>3</sub> thin films. *Journal of Electronic Materials* 2016; 45 (2): 899-909. doi: 10.1007/s11664-015-4209-3
- [41] Lvovich VF. *Impedance Spectroscopy. Applications to Electrochemical and Dielectric Phenomena*, USA: John Wiley & Sons, 2012.
- [42] Bilkan Ç, Azizian-Kalendaragh Y, Altındal Ş, Shokrani-Havigh R. Frequency and voltage dependence dielectric properties, ac electrical conductivity and electric modulus profiles in Al/Co<sub>3</sub>O<sub>4</sub>-PVA/p-Si structures. *Physica B: Condensed Matter* 2016; 500: 154-160. doi: 10.1016/j.physb.2016.08.001
- [43] Dökme İ, Altındal Ş, Gökçen M. Frequency and gate voltage effects on the dielectric properties of Au/SiO<sub>2</sub>/n-Si structures. *Microelectronic Engineering* 2008; 85 (9): 1910-1914. doi: 10.1016/j.mee.2008.06.009
- [44] Pissis P, Kyritsis A. Electrical conductivity studies in hydrogels. *Solid State Ionics* 1997; 97 (1): 105-113. doi: 10.1016/S0167-2738(97)00074-X
- [45] Migahed MD, Ishra M, Fahmy T, Barakat A. Electric modulus and AC conductivity studies in conducting PPy composite films at low temperature. *Journal of Physics and Chemistry of Solids* 2004; 65 (6): 1121-1125. doi: 10.1016/j.jpcs.2003.11.039
- [46] Saghrouni H, Jomni S, Belgacem W, Hamdaoui N, Beji L. Physical and electrical characteristics of metal/Dy<sub>2</sub>O<sub>3</sub>/p-GaAs structure. *Physica B: Condensed Matter* 2014; 444: 58-64. doi: 10.1016/j.physb.2014.03.030
- [47] Coşkun M, Polat Ö, Coşkun FM, Durmuş Z, Çağlar M et al. Electrical modulus and other dielectric properties by the impedance spectroscopy of LaCrO<sub>3</sub> and LaCr<sup>0.9</sup>Ir<sup>0.0</sup>O<sub>3</sub> perovskites. *RSC advances* 2018; 8: 4634-4648. doi: 10.1039/c7ra13261a
- [48] Şafak Y, Asar T, Altındal Ş, Özçelik S. Dielectric spectroscopy studies and ac electrical conductivity on (AuZn)/TiO<sub>2</sub>/p-GaAs (110) MIS structures. *Philosophical Magazine* 2015; 95 (26): 2885-2898. doi: 10.1080/14786435.2015.1081301

- [49] Vural Ö, Şafak Y, Türüt A, Altındal Ş. Temperature dependent negative capacitance behavior of Al/rhodamine-101/n-GaAs Schottky barrier diodes and Rs effects on the C-V and  $G/\omega$ -V characteristics. *Journal of Alloys and Compounds* 2012; 513: 107-111. doi: 10.1016/j.jallcom.2011.09.101
- [50] Yücedağ İ, Kaya A, Tecimer H, Altındal Ş. Temperature and voltage dependences of dielectric properties and ac electrical conductivity in Au/PVC+TCNQ/p-Si structures. *Materials Science in Semiconductor Processing* 2014; 28: 37-42. doi: 10.1016/j.mssp.2014.03.051
- [51] Ladhar A, Arous M, Kaddami H, Raihane M, Kallel A et al. AC and DC electrical conductivity in natural rubber/nanofibrillated cellulose nanocomposites. *Journal of Molecular Liquids* 2015; 209: 272-279. doi: 10.1016/j.molliq.2015.04.020